IEEE Access
Multidisciplinary | Rapid Review | Open Access Journal

Received March 27, 2021, accepted April 9, 2021, date of publication April 13, 2021, date of current version April 21, 2021.

Digital Object Identifier 10.1109/ACCESS.2021.3073030

Adaptive Multi-Input Medium Access Control (AMI-MAC) Design Using Physical Layer Cognition for Tactical SDR Networks

KASHIF SHAHZAD[1], MUHAMMAD UMAR FAROOQ[2], MUHAMMAD ZEESHAN[1], (Member, IEEE), AND SHOAB AHMED KHAN[2]

[1]Department of Electrical Engineering, College of Electrical and Mechanical Engineering, National University of Sciences and Technology, Islamabad 44000, Pakistan

[2]Department of Computer and Software Engineering, College of Electrical and Mechanical Engineering, National University of Sciences and Technology, Islamabad 44000, Pakistan

Corresponding author: Muhammad Zeeshan (ranazeeshan@ceme.nust.edu.pk)

ABSTRACT Tactical software defined radio (SDR) networks demand stringent requirements of latency, throughput, and reliability. In the past, significant efforts have been made to achieve maximal efficiency with modifications and improvements either in an individual layer or through the cross-layer design of its working protocol. In this paper, we propose a novel cross-layer design consisting of adaptive multi-input medium access control (AMI-MAC) layer along with an intelligent channel allocation scheme supported by a multiband multimode physical layer. A cognitive engine further empowers this cross-layer design approach to achieve high throughput, improved quality of service (QoS), and adaptive range capabilities. The proposed physical layer exhibits a mixed use of narrowband and wideband waveforms accommodating different range requirements as per demanded QoS. The uniqueness of the proposed physical layer enables SDR to operate in hybrid topology by receiving multiple narrowband signals of different bandwidths with the same configuration of wideband RF front end. The proposed AMI-MAC design ensures a reduction in both control and data phase latency. MAC layer ensures the maximal utilization of the time and frequency spectrum. Bandwidth and delay optimization is also managed by the proposed trio of the physical layer, MAC, and cognition to reduce latency and achieve desired QoS. Simulation results are presented to show the superiority of the proposed design over conventional tactical radio MAC.

INDEX TERMS Software defined radio, cognition engine, SDR waveform, MAC layer design.

I. INTRODUCTION

Addressing the challenging needs of effective, reliable, and robust communication in a tactical environment has been a very challenging and daunting task. In contrast to the traditional wireless networks, deployment of permanent, immovable infrastructure is neither feasible nor possible in tactical networks due to hostile scenarios. In these intimidating circumstances, software defined radios (SDRs) have been providing efficient, reliable, robust, and secure communication solutions [1]. The task for such self-forming and self-healing intelligent networks provided by SDRs has never been easy as they face the challenges of channel impairments, poor signal-to-noise ratios (SNR), and different service requirements [2]. Physical operational ranges and dynamic data rate requirements are also very abstruse in such scenarios.

The dual challenge of handling the required QoS and variable physical ranges while bandwidth, time, and other resources are limited has been addressed by SDRs in different ways. Several schemes were deployed in the past, where emphasis had been made either on the physical layer alone or the higher layers in conjunction to meet the requirements. Adaptive modulation and coding (ADC) schemes in TDMA and FDMA-based networks were used to improve the data rates [3]. The sole purpose of using any of the modulation schemes in the physical layer is to achieve the desired QoS within the available resources. The SDRs still have to address the range, and data rate paradox [4]. For this purpose, higher layers are utilized to create an appropriate control strategy to maximize the performance with minimal latency.

The associate editor coordinating the review of this manuscript and approving it for publication was Zhenhui Yuan.

To address and manage the data rates for supported ranges, there are two types of waveforms used for SDR implementations, namely narrowband and wideband waveforms [5]. Narrowband waveforms can accommodate longer operational field ranges due to limited bandwidth for given transmitter power. On the contrary, the wideband waveforms can provide higher data rates, but they cannot sustain long-range communication due to absorptions related to shorter wavelengths, and other physical phenomena [6].

An SDR tactical network based on one of the wideband or narrowband schemes cannot achieve a diversity of service qualities and range requirements under variable channel conditions. A heterogeneous ad hoc network with $N = 16$ nodes is shown in figure 1, having meshed connectivity as every node is connected apparently to every other node for communication. This is true as long as all the nodes are operating in the single operative mode and are reachable to each other, i.e., they all are either working on a wideband waveform or a narrowband waveform but not both at a time. This, moreover, is not independent of the range and power constraint. As long as the radios are in closer vicinity to each other, they can have better received power incident at their digital front-ends (DFEs) and support wideband for higher data communication. But if one of the nodes starts to move away, causing an increased distance between the two nodes, they might not be able to operate on the wideband anymore, and hence the away drifting node departs from the network configured to operate in wideband. The classical remedy is that the entire network has to be switched to the narrowband waveform just to accommodate the departing node sacrificing the QoS of the nodes which can still operate on the wider bands.

In figure 1, two arcs expressing the orbital range are shown with reference to node 2. The innermost arc/orbit shows the range supported for wideband communication supporting higher data rate but evidently for a short-range. This means that node 2 can have high data rate communication with nodes 5, 11, and 12 only. The outermost orbit shows the range possible for narrowband communication. Hence, node 2 can have low data rate communication with all other nodes. This may be suitable if nodes are required to communicate at lower data rates. If high throughput or low latency are required, the fixed-bandwidth network fails to address the service needs, compromising the required QoS.

The first value addition to the given scenario is by the physical layer being presented. Due to the support of operating variable bands in narrowband, different data rates can be offered to different radios simultaneously. This is shown by showing another arc in the middle (see figure 2. For exemplary purposes, it is shown that low, medium, and high data rates can now be offered as three different types of bandwidths are in utilization instead of restraining to a fixed narrowband or wideband. With the addition of another value band of operation, nodes 1, 7, 10, 15, 13, and 6 can communicate with node 2 on medium data rates. This resolves two main issues in the stated ad hoc network. Firstly, the network

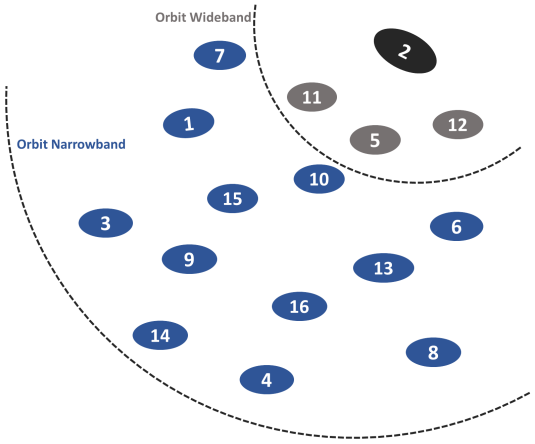

FIGURE 1. SDR tactical network comprised of 16 nodes supporting two bandwidths.

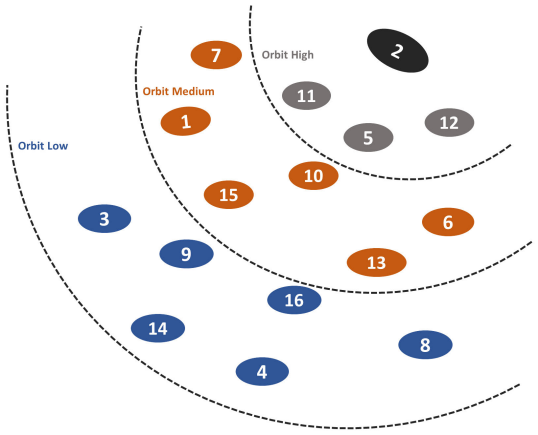

FIGURE 2. SDR tactical network comprised of 16 nodes supporting multiple bandwidths.

does not have to operate strictly on one waveform just to accommodate the drifting node. It can operate simultaneously multiple bands (three for the figure 2). This not only gives a hybrid touch to the network but also provides diversified data rates with range accommodation. Secondly, the mobile node drifting away from the main mesh does not have to exit but can drop down to the lower band and, in turn, the lower rates without bothering the date rates and band of the other nodes.

This paper presents a novel cross-layer AMI-MAC design capable of achieving data efficiency through a smart channel allocation mechanism. The proposed AMI-MAC is augmented by the physical layer with a diversity of simultaneously using narrowband and wideband waveforms through a common RF front end. The baseband electronics supports multiple signal processing branches in parallel due to the advent of multicore processors used in SDR. This not only addresses the narrowband signals of different bandwidths to be received and processed by multiple users but also addresses the different QoS for different ranges using information from the cognitive engine. The cognitive engine provides a complete insight of resource on-demand (RoD) for the MAC layer to be built around it. The same RF

stage can also receive and process the wideband waveforms if high data rates are required switching to the wideband mode of SDR. With this physical layer, SDR possesses the adaptive capability to process whatever arrives at the RF stage regardless of its waveform within the defined upper bound of available spectral bandwidth. This enables the SDR to switch between variants of narrowband and wideband mode with defined constraints.

A. RESEARCH CONTRIBUTIONS

A novel AMI-MAC cross-layer design is proposed for ad-hoc tactical networks, which fully benefits from our previously proposed physical layer design [4] with coordination from the suggested cognitive engine. A key contribution of the proposed MAC minimizes the control allocation time multifold, especially in a larger network reducing the latencies inherent to the control allocation phase. The design offers the following major contributions to the research field and SDRs as a network.

1) A novel concept of receiving narrowband and wideband signals simultaneously with a common RF front end.
2) Provision to receive and process multiple narrowband signals of different bandwidths providing multi-narrowband multiuser SDR.
3) Addressing different near and far range requirements with the help of proposed cognitive engine to choose between available waveforms based on RoD.
4) Minimization of network latency and service-based data slot allocations through proposed AMI-MAC for tactical radio networks

II. PROBLEM FORMULATION

A hybrid NB/WB waveform that can handle radio range requirements, provide simultaneous diverse data rates, maintains reduced control phase to minimize latency, and improves throughput must be aware of underlying channel conditions to satisfy certain service requirements. Range requirements are indicated by the underlying channel conditions like received signal strength indicator (RSSI) and signal to noise ratio (SNR), which are only available at the physical layer. Service requirements (data rate/size) are only known to the link layer; therefore, service on-demand can only be addressed at MAC. Simultaneous multicarrier reception at the physical layer can significantly reduce latency and increase throughput by enabling multiple collision-free transmissions in the same control/data slots. MAC is unaware of the underlying physical layer parameters and operates as a separate layer on top of the physical layer.

This gives rise to the need for a cognition engine that can select suitable bandwidth and mode of operation based on specific input parameters applicable to the hybrid NB/WB waveform. With help from an available cognitive engine, a comprehensive cross-layer MAC can enable the co-existence of radios that can listen to multiple simultaneous transmissions, communicate at different distances/bands depending upon the service requirements.

III. RELATED WORK

Adaptation of RF receivers in SDRs to support multiple operation modes is a tedious task as to reconfigure the analog components is practically complicated [7]. Therefore, the flexibility is accomplished by reconfiguring the DFE, which changes the programming parameters of various embedded platforms and digital mixers [8], [9]. Different signal processing blocks can be shared by using DFE, facilitating the RoD, channel instantaneous conditions, and wireless communication models [10]. [11] reports an adaptive DFE-based wireless receiver in which multiple modes of operation through sharing of multiple stages of DSP. Another scheme is presented in [12] to facilitate various demands based on load and channel in the uplink of code division multiple access (CDMA). It uses sequential optimization for the resource allocation of multiple nodes. A fuzzy inference-based scheme for link adaptation in burst mode wideband networking waveform of SDRs is presented in [13]. The aim is to reduce the overhead caused due to re-transmission through the cognition of transmission characteristics of transmitter and receiver based on channel variations and user QoS requirements for multicode CDMA in the physical layer. With the aim of maximizing energy yield, a dynamic scheme for the adaptation of bandwidth, constellation size, transmit power, and antenna arrangement is proposed in [14] while complying with the desired service quality.

A hybrid scheme for parameter adaptation is introduced in [15]. The proposed algorithm combines adaptive modulation and coding (AMC) and automatic repeat request (ARQ) at the physical and data link layers, respectively, maximizing the transmission data rate in cognitive radio (CR). Performance of cognitive throughput is governed by packet loss rate (PLR), and minimum throughput required. A cross-layer approach to solve the link adaptation problem is proposed in [16] applicable to a wireless network consisting of multiple users having multimedia traffic. In [17], based on stability analysis, authors have suggested the order-based frequency allocation in the case of CR. An algorithm for band allocation to secondary cognitive users and the stability analysis of the network layer is proposed in [18] based on the stability of their queue's demand. A scheme based on distributed sensor network to identify uninvited entering drones is proposed in [19]. The approach also evaluates their geographical positions. Using an integrated framework of SDRs and optimization algorithms, the system proposed in [19] facilitates connectivity of SDRs placed at different geographical locations through multiband and multimode capability. In [20], authors have developed a receiver to process signals from multiple narrowband users. The limitation of this approach is that it is strictly based on continuous phase modulation (CPM). Based on IP networks, cross-layer optimization schemes are proposed in [21], [22]. A scheme for joint optimization of

network resources and data center responsiveness is proposed to achieve desired service requirements. In [22], authors have proposed a cross-stratum optimization (CSO) architecture for achieving the QoS demands.

A cross-layer framework to provide collision-free communication, reduce delays, and reuse empty time slots in SDR tactical networks is proposed in [23]. The authors have proposed a cross-layer mechanism to support routing and MAC. Another algorithm to improve network throughput and reduce delays is presented in [24] by using a hybrid TDMA/FDMA approach. Specifically, a multi-channel MAC protocol is provided to schedule the time slots for SDRs. Authors have proposed optimized use of control packets to overcome control message overhead. For multi-hop tactical networks, a mathematical model for cross-layer design to optimize the performance of SDR tactical networks is proposed in [25]. The aim is to improve energy efficiency, enhance network throughput and reduce latency. A common limitation of these cross-layer algorithms is that they are neither aware of the physical layer parameters nor consider multiple bandwidth support.

After extensive literature review, one or more of the following limitations have been found to the best of our knowledge; (1) Either the analysis is focused on parameter's adjustments only for either wideband or narrowband waveform, (2) a sequential control phase is followed where every radio transmits in its allocated time slot, and (3) multi-input, variable bandwidth support in the cross-layer design is not considered. The objective of this paper is to overcome these problems through an efficient and adaptive multi-input cross-layer PHY/MAC design capable of processing multiple signals requiring diverse service quality for both long and short-range communication in tactical SDR networks.

IV. PROPOSED HYBRID NB/WB PHY LAYER

In this section, we present the proposed hybrid NB/WB physical layer design based on multiple bands and modes of operation. A top-level physical layer of hybrid narrowband/wideband waveform is presented in our previous work [4]. The main objective is to support parallel transmission and reception of multiple signals having the same or different bandwidths. Through the use of DFE, the required functionality is achieved with minimal changes in the wideband analog front-end (AFE). A composite signal is formulated after digital mixing of various signals. This composite signal is transmitted in the wideband mode of the SDR waveform. On the receiver side, after passing through the wideband AFE, separate signal processing and filtering of each of the corresponding signals is performed. One of the main advantages of this proposed approach is the capability to process multiple signals with different bandwidths according to the service quality and range specifications through the same wideband front end.

Figure 3 exhibits a composite of multiple signals in the frequency domain having different bandwidths. Theoretically, bandwidth can take on any value between 0 to $B_{RF} = f_b - f_a$, but practically there will be some finite choices of bandwidth

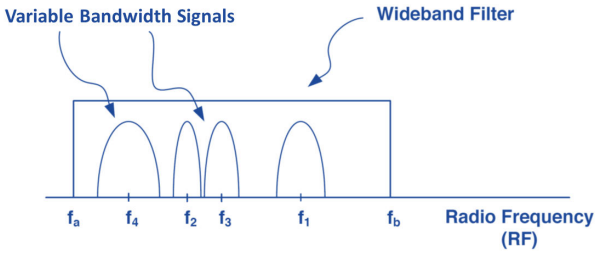

FIGURE 3. A composite of four signals having different bandwidths.

available for any user. The narrow bandwidths are divided into three categories, namely low bandwidth (B_L), medium bandwidth (B_M), and high bandwidth (B_H). The wide bandwidth is denoted by B_{BW}. Inside an analog wideband RF bandwidth, available number of low, medium, high and wideband channels are n_L, n_M, n_H, and n_{WB}, respectively, where $n_L > n_M > n_H > n_{WB}$. The processing flow of the proposed hybrid NB/WB scheme is shown in figure 4. After passing through analog WB front-end and ADC, the data for each user is processed in parallel through digital mixing, variable bandwidth filtering, and demodulation.

One of the crucial steps is the selection of an appropriate baseband modulation scheme for narrowband and wideband modes of the proposed waveform. Two key factors that need to be considered for this selection are: (1) the modulated signal should be robust to additive noise and channel impairments, (2) the modulated signal should be bandwidth efficient. Keeping in view these two factors, we have chosen continuous phase modulation (CPM) and filterbank multicarrier (FBMC) as the modulation schemes for narrowband and wideband modes, respectively.

A. CPM: NARROWBAND MODULATION SCHEME

Continuous phase modulation (CPM) is chosen for a narrowband mode of the proposed waveform physical layer due to its constant envelope and continuous phase, which makes it noise resilient and spectral efficient. The modulated signal of CPM [4] is given by

$$s(n) = \sqrt{\frac{2E}{T}}\ cos(2\pi f_c n + \phi(\underline{a}, n)) \tag{1}$$

where

$$\phi(\underline{a}, n) = 2\pi h \sum_{i=-\infty}^{\infty} a_i q(t - iT) \tag{2}$$

with

$$q(t) = \int_{-\infty}^{t} g(\tau) d\tau \tag{3}$$

Here, $g(t)$ is a pulse shaping filter that is selected to attain desired smoothness in the transmitted data [26]. Also, f_c is the carrier frequency, T is the signaling duration, E is the symbol energy. In each time interval, $\phi(\underline{a}, n)$ results in a specific pattern for each M-ary symbol. Pulse shaping filter type is chosen to obtain the desired level of continuity in the

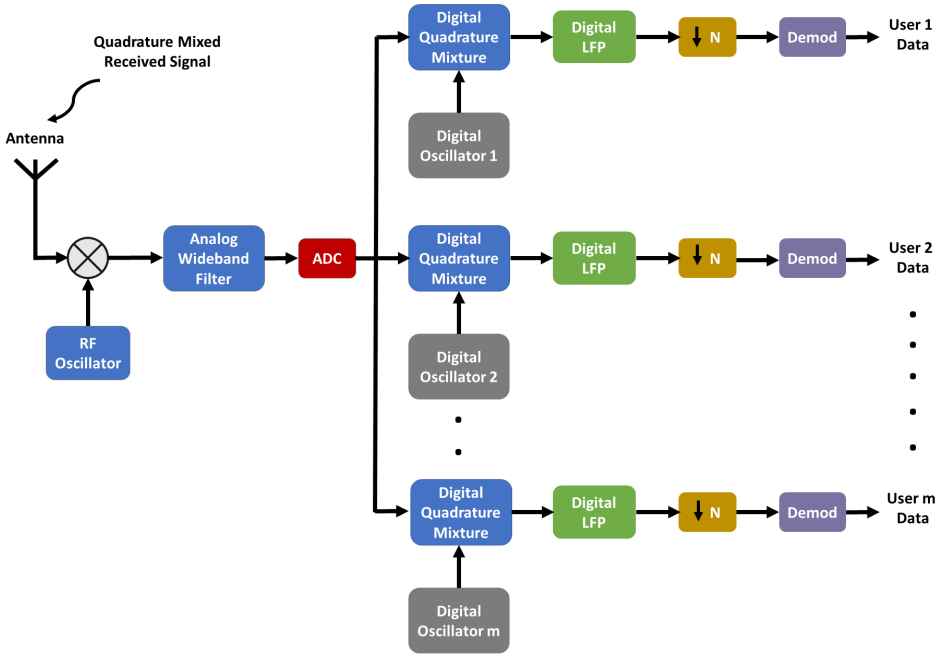

FIGURE 4. Processing flow of the proposed NB/WB Scheme.

TABLE 1. Proposed narrowband transmission modes within a single bandwidth of 100 kHz.

Mode	M	h	L	Data Rate (kbps)
Mode 1	8	1/2	2	69.6
Mode 2	4	1/2	3	92.4
Mode 3	8	1/4	2	120.8
Mode 4	4	1/4	2	151.4
Mode 5	4	1/8	1	181
Mode 6	4	1/8	2	190
Mode 7	8	1/8	3	201.6
Mode 8	8	1/16	2	274.8
Mode 9	4	1/16	1	317.4
Mode 10	4	1/16	2	352.4

resulting CPM signal. Based on different possible values of modulation index (h), modulation order (M), and overlapping factor (L), a multiband multimode CPM scheme is proposed, and multiple modes of operation by varying transmission bandwidth are generated according to the applications and service requirements. For each bandwidth, several modes of operation are proposed to achieve different throughputs as required by a particular user. Table 1 shows 10 modes of operation for 100 kHz bandwidth with data rate ranging from 69.6 kbps to 352.4 kbps. A similar approach can be followed to devise other modes for the finite choices of bandwidth mentioned earlier.

B. FBMC: WIDEBAND MODULATION SCHEME

For the wideband mode of the proposed waveform, filterbank multicarrier (FBMC) is selected as the underlying modulation scheme for the proposed physical layer design. FBMC is one of the advanced modulation schemes being used in 5G communication technology. To reduce the intercarrier interference (ICI) and improve the spectral efficiency, synthesis filter bank (SFB) and analysis filter bank (AFB) are used, which are the frequency-shifted versions of low pass prototype frequency response [27], [28]. A highly selective filter is obtained from the prototype filter response constituting $2\Gamma - 1$ pulses in the frequency domain with the help of specifically defined frequency coefficients, where Γ is the ratio of the filter impulse response to the multicarrier symbol duration or the number of samples the overlap in the time domain. The impulse response of the filter [29] is given by

$$h(t) = 1 + 2\sum_{k=1}^{\Gamma-1}(-1)^k H\left(\frac{k}{L}\right)\cos\left(\frac{2\pi km}{L}\right) \qquad (4)$$

here,

$$m = 1, 2, 3, \ldots, L-1$$

L is the prototype filter length and could be of any choice among $L = \Gamma M$, $L = \Gamma M + 1$ or $L = \Gamma M - 1$, where the total number of subcarriers is given by M.

In FBMC physical layer, after the addition of redundancy in the source data with the help of convolutional encoding, the data is modulated with QAM modulation. Subsequently, the serial to parallel conversion and OQAM modulation by segregating complex modulated symbols into real and imaginary components in order to gain overall exploitation of channel bandwidth [30], [31] is performed. Finally, the modulated data symbols are passed through IFFT-based SFB and sent to DFE. On the receiver side, the data is first passed through

TABLE 2. Proposed wideband transmission modes for bandwidth of 1 MHz.

Mode	M	r	Data Rate(Mbps)
Mode 1	2	1/2	0.5
Mode 2	2	1/3	0.67
Mode 3	4	1/2	1
Mode 4	4	1/3	1.33
Mode 5	8	1	2

the FFT-based AFB. After that, OQAM post-processing is done where the data that was split into real and complex parts are recombined again and converted back to serial data from the incoming parallel streams. In the end, the data is decoded utilizing the Viterbi decoder as a counterpart of convolutional encoding employed on the transmitting side.

By using different values of modulation order (M), subcarrier count (N), and code rate (r), multimode FBMC scheme is proposed, and multiple modes of operation by varying transmission bandwidth are generated according to the service requirements. Each mode of operation results in different throughput, which helps to select a suitable mode of operation as per user requirement. Table 2 shows 5 modes of operation for RF bandwidth of 1 MHz with data rate ranging from 0.5 Mbps to 2 Mbps. It is worth mentioning here that user throughput is independent of the subcarrier count; however, the performance of FBMC is improved by increasing the number of subcarriers. Due to this reason, it is taken as an output from the cognition engine but not used for the computation of theoretical throughput in table 2.

V. PROPOSED COGNITION ENGINE

The proposed cognitive engine (see figure 5) is a facilitating layer of intelligence between the physical layer and MAC. It ensures the maximal utilization of the proposed PHY for addressing several service parameters. It translates the channel state based on RSSI and SNR as a function of range between SDR nodes and evaluates it against the demanded data service. Based on the underlying channel conditions, it approves or disapproves service requests as per underlying channel conditions. This enables the cognitive engine to choose between the available waveforms and select appropriate parameters required by the waveform selected for desired QoS in the data phase. For the control phase, it passes the information of simultaneous requests made by the other nodes in addition to the actual request made by the source node. This enables the MAC to reserve and not to use the time slots of higher priority nodes in the control phase. The proposed MAC, to be explained in the subsequent section, selects the slots for the data phase and updates to the cognition engine, which further informs PHY to transmit data in its due turn during the data phase.

VI. PROPOSED AMI-MAC ALGORITHM

This section presents a novel intelligent MAC layer design that can benefit from the cognitive engine and physical layer

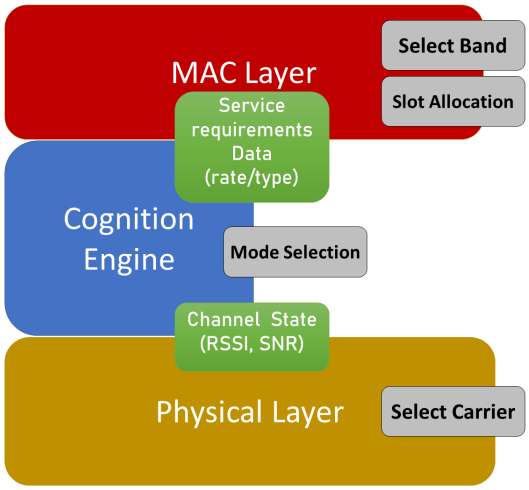

FIGURE 5. Proposed cognition engine.

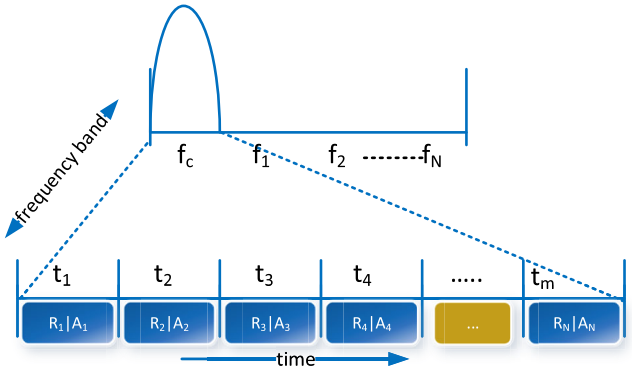

FIGURE 6. An overview of classical tactical radio MAC.

presented in the previous sections. The physical layer directly controls link parameters required for range/data rate management, whereas, MAC layer is aware of the demanded service quality. Therefore, an intermediate cognitive engine layer is introduced to facilitate the seamless exchange of parameters. This feature facilitates the MAC layer for selecting appropriate band/time slots to achieve desire service quality. To highlight the significance of the proposed cross-layer design, initially, a discussion on traditional SDR MAC is presented to explain the usage of single-input narrowband fixed-bandwidth frequencies along with allocation of data slots in TDM/FDM based tactical ad hoc networks. This mechanism is termed as classical tactical radio MAC (CTR-MAC). After that, the proposed adaptive multi-input MAC (AMI-MAC) for time and frequency efficient channel allocation is presented. In the proposed scheme, multiple control frequencies are utilized with variable-bandwidth support for data slots, capitalizing on the strong hybrid physical layer presented in previous sections. The proposed scheme is far more promising, based on practicality, and possesses completeness in design from the physical layer to MAC implementation.

A typical tactical radio network operates on either a narrowband or a wideband waveform, with fixed-bandwidth

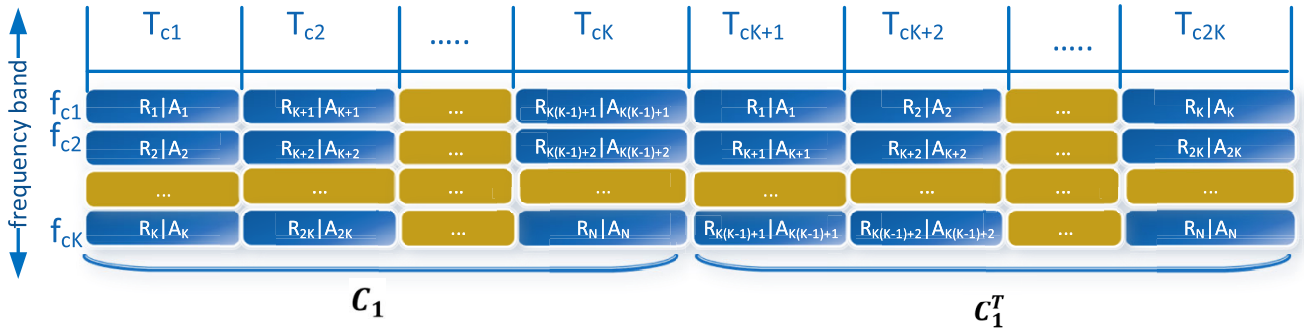

FIGURE 7. Proposed time-frequency matrix for AMI-MAC.

slices called bands. There can be several bands, but the bandwidth for communication is fixed, e.g., NATO forces use a standard 25 kHz band for narrowband communications. One band is reserved for the transfer of control information during the control phase, while other bands are used for data exchange between radios during the data phase. Control and data phases are usually time-slotted and repeat one after the other. Time slot/band agreements for data transfer during the data phase are carried out in the control phase. Figure 6 depicts a generic CTR-MAC with N bands and m time slots. The band f_c is used to transfer control information, while other bands from f_1 to f_N are used for data exchange between radios. Any radio can transmit at a single band during its allotted time slot. The use of a hybrid TDM/FDM MAC design is preferred for distributed tactical radio networks for their mission-critical nature, as such designs can offer service guarantees (latency, data rate, etc.). However, this significantly limits network size. Enhancements like subnet formations for group communications, contention over control slots, master-slave configurations, splitting control phase across multiple data phases, and equipping nodes with multiple radio interfaces are often used to improve network's performance.

Unlike CTR-MAC, the proposed AMI-MAC design benefits from the physical layer and cognitive engine stated previously to provide simultaneous reception of multiple signals, multiple simultaneous transmissions in the control phase, variable-sized bands, and co-existence of narrowband/wideband waveforms. The freedom of receiving multiple signals eliminates the restriction for radio to tune to a single frequency for either control or data channels. This parallel processing capability can be used in multiple ways for a tactical network to achieve significant performance enhancements. The stated physical layer can even provide the opportunity to handle and process control and data channels simultaneously, but upon evaluation, this approach creates several bottlenecks.

The scheme stated here keeps separate control and data phases. Both control and data phases allow the reception and processing of multiple simultaneous bands. During the control phase, a subset of radios makes a request during the same time slot. Each requested node allocates a band and time slot via an allocation message issued during the same slot. In subsequent slots, the next subsets of radios transmit request messages. The request/allocation-based time-slotted control phase is depicted in figure 7. For an N radio network, the design suggests using $K = \sqrt{N}$ simultaneous transmissions using bands $f_{c1}, f_{c2}, \ldots, f_{cK}$. This reduces the number of required time slots to K, forming a $K \times K$ time-frequency matrix $\mathbf{C_1}$. Since the transmitting nodes cannot receive requests made to them, the transpose of the above-mentioned matrix is also concatenated to the control phase. This results in $2K$ time slots for the control phase, making dimensions of the time-frequency matrix ($\mathbf{C} = [\mathbf{C_1}|\mathbf{C_1^T}]$) for the control phase to $K \times 2K$. For instance, the proposed design requires only 16 time slots for a 64-radio network that significantly lowers control-phase latency.

For service-oriented slot allocations in the data phase, nodes are prioritized in the reverse order of their IDs, i.e., node 1 has a higher priority than node 2. For the data phase, the time slots and bands are selected by the requested nodes on the basis of priority. The spectrum is divided into several variable-sized bands, ranging from low to high as per the available RF bandwidth discussed in PHY. For each band, multiple time slots, T_D can be allocated according to the service needs. Let $N_{T,L}$, $N_{T,M}$, $N_{T,H}$, and $N_{T,WB}$ be the number of data slots reserved for low, medium, high, and wideband modes, respectively, to meet the service needs. Thus, the maximum size of data phase is $max(N_{T,L}, N_{T,M}, N_{T,H}, N_{T,WB}) \times K$. The actual number of time slots consumed is generally less than the maximum size of the data phase, and MAC can shrink the data phase to reduce latency. A radio receives all request messages transmitted in the request phase of each control slot and reserves slots in requested bands subject to confirmation from the cognitive engine. The reservation process tries to consume minimum time slots by exhausting the available bands first and then the time slots. The radios addressed in the request phase reserve allocation slots for the data phase with help from the cognitive engine. This reservation is announced via allocation message during the same time slot. Radios listening to the allocation messages update their time-frequency matrix for the data phase. The

Algorithm 1: Control Phase (Request Message)

Notations:

1) N: Network size
2) $K = \lceil \sqrt{N} \rceil$: Number of control channels
3) $B_\alpha = \{B_{\alpha,1}, B_{\alpha,2}, \ldots, B_{\alpha,n_{ch}}\}$: Class of different bandwidth channels, where $\alpha \in \{L, M, H, WB\}$ and $n_{ch} \in \{n_L, n_M, n_H, n_{WB}\}$
4) $B = \{B_L \cup B_M \cup B_H \cup B_{WB}\}$: Set of band classes
5) $F_c = \{f_{c1}, f_{c2}, \ldots, f_{cK}\}$: Set of control frequencies
6) $N_{T,\alpha}$: Number of data slots reserved for channel type $\alpha \in \{L, M, H, WB\}$
7) $\Delta = max(N_{T,\alpha}) \times K$: Data frame size
8) T_{Dm}: m^{th} data slot, where $m = 1, 2, \ldots, \Delta$
9) $\mathbf{C} = [\mathbf{C_1}|\mathbf{C_1^T}]$: Time-frequency matrix of order $K \times 2K$, and $\bar{\mathbf{c}}_l$ be the l^{th} column vector of matrix $\mathbf{C}$ defined by $\bar{\mathbf{c}}_l = [1 + (l-1)K, \ldots, K + (i-1)K]^T$

Initialization: Choose N, B_α, $N_{T,\alpha}$
for $(i = 1 : N)$ **do**
  if *(node* $i \in \bar{\mathbf{c}}_l$ *& node i has data to transmit)* **then**
    Send request message ;
  else
    Process received request messages ;
    // Set time-frequency matrix $\mathbf{C}$;
    for $(k = 1 : K)$ **do**
      Set slot $m = 1$, // Find available slots in requested band class α ;
      while $m \leq \Delta - N_{T,\alpha}$ **do**
        for $(j = 1 : n_{ch})$ **do**
          if *(T_{Dm} to $T_{D(m+N_{T,\alpha}-1)}$ are available)* **then**
            Select j^{th} channel ;
            Break;
          else
            $m = m + N_{T,\alpha}$;
          end
        end
      end
      if $(j \neq 0)$
      Reserve T_{Dm} to $T_{D(m+N_{T,\alpha}-1)}$ for $B_{\alpha,j}$ in data phase communication table ;
      end if
      if (i is the requested node)
      Choose PHY mode in accordance with service quality & range ;
      if *QoS possible* **then**
        Send ACK in allocation packet ;
      else
        Send NACK in allocation packet ;
      end
      end if
    end
  end
end

Algorithm 2: Control Phase (Allocation Message)

for *Each allocation message received during* $\bar{\mathbf{c}}_l$ **do**
  if *(node* $i \in \bar{\mathbf{c}}_l$*)* **then**
    if *(ACK received)* **then**
      Read allocation message schedule ;
      Update data phase communication table ;
    else
      if (node i is the intended destination)
      if *(Lower service quality acceptable)* **then**
        Create a required message with lower service requirements ;
      else
        Request routing layer for multi-hop communication ;
      end
      end if
    end
  else
    Update data phase communication table ;
  end
end

TABLE 3. Control phase transmission table using time-frequency matrix for $N = 16$.

	T_{c1}	T_{c2}	T_{c3}	T_{c4}	T_{c5}	T_{c6}	T_{c7}	T_{c8}
f_{c1}	1	5	9	13	1	2	3	4
f_{c2}	2	6	10	14	5	6	7	8
f_{c3}	3	7	11	15	9	10	11	12
f_{c4}	4	8	12	16	13	14	15	16

proposed AMI-MAC design is depicted in algorithms 1 and 2, followed by a thoroughly explained working example.

VII. WORKING EXAMPLE

In this section, we present the working example of the proposed solution with a mesh network of 16 SDR nodes, i.e., $N = 16$. As per the proposed algorithm, for the control phase, the nodes will be prioritized and arranged in a time-frequency matrix for which $K = \sqrt{N} = \sqrt{16} = 4$. The example taken is a mesh network where all nodes are connected to each other, but for the sake of simplicity, some level of connectivity is shown between certain nodes through dotted lines. It is explained in the previous sections that the frames appear in the cycles of control and data frames. The control frame will be formed by using the time-frequency matrix $\mathbf{C}$ with dimensions of $K \times 2K = 4 \times 8$. Therefore, the time slots T_{c1} to T_{c8} will be used for the request/allocation phase of 16 radios with 4 simultaneous bands with carrier frequencies from f_{c1} to f_{c4}. This distribution of nodes for the R|A phase is shown through the time-frequency matrix in table 3.

The priority of nodes is in descending order, i.e., node 1 has higher priority than node 2, while node 2 has higher priority

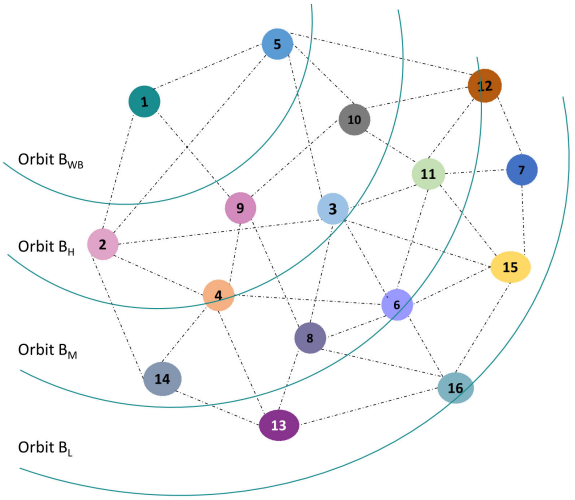

FIGURE 8. Range orbits with respect to node 1.

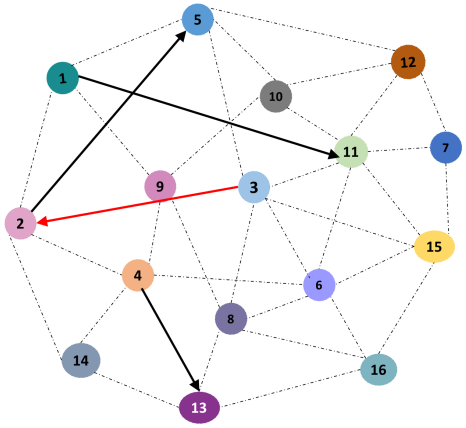

FIGURE 9. Nodes representing R|A phase for T_{c1}.

TABLE 4. R|A phase for T_{c1}.

Tx Node (Request)	Rx Node (Allocation)	Data Rate
1	11	Low
2	5	Low
3	2	Low
4	13	Medium

than node 3, and so on. In this control phase, the time slots and frequency bands will be selected by the requested node on the basis of priority as per the algorithm by the cognitive engine. For this example, we are assuming the division of spectrum such that, $n_L = 8$, $n_M = 4$, $n_H = 2$ and $n_{WB} = 1$. This means that for one specific node, other nodes lie in one of the four ranges where communication in one of the four band classes is possible. This is shown in figure 8 with the help of the orbits B_L, B_M, B_H and B_{WB}, with respect to node 1.

As per figure 8, node 1 can communicate with node 5 using wideband class while maintaining communication with node 8 using medium band class and with node 15 using low band class, simultaneously. In this example, we have assumed that there is no denial of service and communication is possible between all nodes, at least in narrowband mode. This provides us a distribution of frequency bands for data as $B_{L,1}$ to $B_{L,8}$, $B_{M,1}$ to $B_{M,4}$, $B_{H,1}$, $B_{H,2}$ and $B_{WB,1}$. The number of time slots are taken as $N_{T,L} = 4$, $N_{T,M} = 3$, $N_{T,H} = 2$ and $N_{T,WB} = 1$. The maximum number of data slots is $\Delta = 16$, and thus we can have the time slots for data from T_{D1} to T_{D16}. The usual number of time slots consumed during the data phase is generally much lesser than Δ.

In the first time slot of control phase T_{c1}, nodes 1,2 3 and 4 will simultaneously transmit making requests to the required nodes of 11, 5, 2 and 13 respectively as shown in figure 9 and table 4. The request phase of nodes 1,2,3 and 4 are aligned and cannot listen to the requests they are simultaneously making. However, in the allocation phase, they can listen to the acknowledgments being made to them. The request made by node 1 will be received by all the other nodes, including the originally intended node 11. Since node 1 has higher priority than other nodes requesting in T_{c1}, therefore node 5 and 13 will assume that the service will either be acknowledged or denied, so they will not take the slots being reserved for node 1→11. Since node 1 has requested a low data rate service from node 11, the cognitive engine will check the underlying channel conditions and evaluate if the communication is possible or not. As explained earlier, we are not considering the denial of service; therefore, node 11 can communicate with node 1 on low data rates.

Cognitive engine of node 11 will accept the request and will inform MAC which will allocate the first 4 time slots in $B_{L,1}$ being the first available band. T_{D1} to T_{D4} in $B_{L,1}$ will be allocated for 1→11. This acknowledgment from node 11 to 1 is also received by nodes 2,3 and 4, which keeps the allocation table updated. Node 2 has requested node 5 for low data rate communication. Node 5, through its physical layer, has already listened to the request of node 1 made to node 11. Even though node 5 does not know about the reply of node 11 to 1, as it also has to acknowledge at the same time when the acknowledgment from 11 to 1 is being made. It is aware of the requested data rate and considers the slots occupied based on priority. As per the algorithm, the first 4 available slots in $B_{L,1}$ are reserved for 1→11 and will not use them. The next available slots for node 5 to acknowledge are T_{D1} to T_{D4} in $B_{L,2}$. Node 3 requesting to node 2 is not possible as both radios are in R|A phase. Node 4 requesting medium data rate to node 13 will be addressed by allocating T_{D1} to T_{D3} of $B_{M,1}$ being the first available medium band class.

In time slot T_{c2}, nodes 5,6,7 and 8 will request their intended destinations as shown in figure 10 and table 5. Node 5 will request node 2 for low data rate and will be awarded the time slots T_{D5} to T_{D8} in $B_{L,1}$. This is because T_{D1} to T_{D4} are the time slots, in which node 2 is in transmission mode. Therefore, it cannot take the next low band $B_{L,3}$ in T_{D1} to T_{D4} referred to as the conflict of transmission. Node 15 will allocate T_{D1} to T_{D4} in $B_{L,3}$. Node 14 will allocate T_{D1} and T_{D2} to node 8 for high-rate communication in $B_{H,1}$. The wideband requested by node 7 to node 11 will be addressed in $B_{WB,1}$ as node 11 is already in the receiving mode. This performance

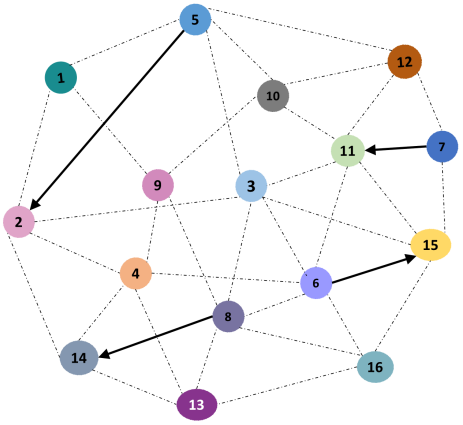

FIGURE 10. Nodes representing R|A phase for T_{c2}.

TABLE 5. R|A phase for T_{c2}.

Tx Node (Request)	Rx Node (Allocation)	Data Rate
5	2	Low
6	15	Low
7	11	Wideband
8	14	High

gain in data phase is achievable through proposed cross-layer design.

The combined T_{c3} and T_{c4} scenario is shown in figure 11 and table 6. In control time slot T_{c3}, nodes 9, 10 and 11 are all requesting to node 3 for medium mode communication while node 12 is requesting node 7 for low data rate. T_{D1} to T_{D3} are allocated for 9→3 and 10→3 communication on $B_{M,2}$ and $B_{M,3}$ respectively. Since node 11 is in reception mode in first four time slots therefore, it gets T_{D5} to T_{D7} on $B_{M,1}$ as first available option based on its priority. Avoiding the conflict of transmission, node 7 allocates T_{D2} to T_{D5} for 12→7 communication. In T_{c4}, requests made by node 13 to 16 and node 15 to 13 are not possible due to simultaneous R|A phase. Node 14 has requested high data rate service from node 8, while node 16 has requested low band class from node 1. T_{D3} and T_{D4} are allocated by node 8 for 14→8 communication on $B_{H,1}$ while T_{D5} to T_{D8} are allocated for 16→1 on $B_{L,2}$.

By the end of T_{c4}, all the 16 nodes have gone through their R|A phase at least once. It is evident that the requests made by node 3 to 2, node 13 to 16, and node 15 to 13 were not possible as they were in simultaneous R|A phase being in the current T_c. The issue is resolved in the remaining part of the control phase, where the transposed version of this 4×4 matrix is concatenated as explained in the algorithm. The composite control time slots T_{c5} to T_{c8} are shown in the figure 12 where the remaining unallocated nodes complete their R|A phase. It is worth mentioning that any denial of service allows the requesting node to lower the service needs or benefit from the routing algorithm at the network layer, according to the application requirements.

In T_{c5}, there is no request made by node 1,5 or 9 but node 13 will make the pending request to node 16 for low-rate

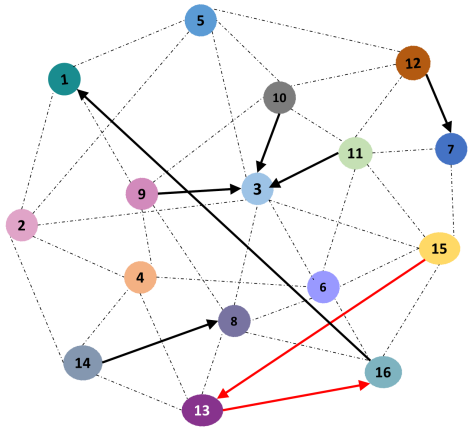

FIGURE 11. Nodes representing R|A phase for T_{c3} and T_{c4}.

TABLE 6. R|A phase for T_{c3} and T_{c4}.

Tx Node (Request)	Rx Node (Allocation)	Data Rate
9	3	Medium
10	3	Medium
11	3	Medium
12	7	Low
13	16	Low
14	8	High
15	13	Low
16	1	Low

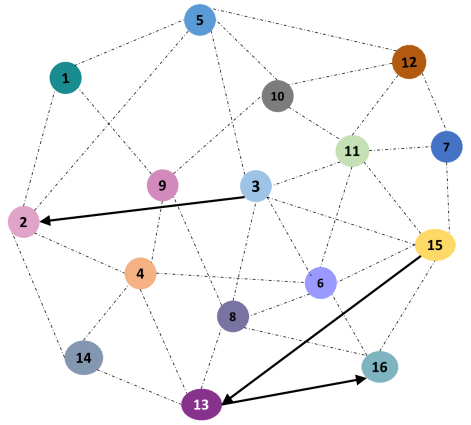

FIGURE 12. Nodes representing R|A phase for T_{c5} to T_{c8}.

communication and will be awarded slots T_{D9} to T_{D12} in band $B_{L,1}$ (see figure 12). There is no request or allocation made in T_{c6}. In T_{c7}, node 3 will request node 2 for low data rate and will be acknowledged by allocating the time slots T_{D8} to T_{D11} in $B_{L,3}$. There is no request made by node 7 and 11 in this time slot. Node 15 will request node 13 and will be allocated slots from T_{D5} to T_{D8} in $B_{L,5}$. Since all the nodes have made their requests and allocations, therefore there is no R|A made in T_{c8}. The entire R|A phase updated matrix for T_{c1} to T_{c8}, and spectrum allocation for data phase are shown in the tables 7 and figure 13. Here the notation

$$R^{q}_{p,\alpha}|A^{p,T_{Dm_1}:T_{Dm_2}}_{q,B_{\alpha,j}}$$

TABLE 7. Request|allocation table for $N = 16$.

	T_{c1}	T_{c2}	T_{c3}	T_{c4}	T_{c5}	T_{c6}	T_{c7}	T_{c8}
f_{c1}	$R^{11}_{1,L}\|A^{1,T_{D1}:T_{D4}}_{11,B_{L,1}}$	$R^{2}_{5,L}\|A^{5,T_{D5}:T_{D8}}_{2,B_{L,1}}$	$R^{3}_{9,M}\|A^{9,T_{D1}:T_{D3}}_{3,B_{M,2}}$	$R^{16}_{13,L}\|A^{\times}_{\times}$	$R^{\times}_{1}\|A^{\times}_{\times}$	$R^{\times}_{2}\|A^{\times}_{\times}$	$R^{2}_{3,L}\|A^{3,T_{D8}:T_{D11}}_{2,B_{L,3}}$	$R^{\times}_{4}\|A^{\times}_{\times}$
f_{c2}	$R^{5}_{2,L}\|A^{2,T_{D1}:T_{D4}}_{5,B_{L,2}}$	$R^{15}_{6,L}\|A^{6,T_{D1}:T_{D4}}_{15,B_{L,3}}$	$R^{3}_{10,M}\|A^{10,T_{D1}:T_{D3}}_{3,B_{M,3}}$	$R^{8}_{14,H}\|A^{14,T_{D3}:T_{D4}}_{8,B_{H,1}}$	$R^{\times}_{5}\|A^{\times}_{\times}$	$R^{\times}_{6}\|A^{\times}_{\times}$	$R^{\times}_{7}\|A^{\times}_{\times}$	$R^{\times}_{5}\|A^{\times}_{\times}$
f_{c3}	$R^{2}_{3,L}\|A^{x}_{x}$	$R^{11}_{7,WB}\|A^{7,T_{D1}}_{11,B_{WB,1}}$	$R^{3}_{11,M}\|A^{11,T_{D5}:T_{D7}}_{3,B_{M,1}}$	$R^{13}_{15,L}\|A^{\times}_{\times}$	$R^{\times}_{9}\|A^{\times}_{\times}$	$R^{\times}_{10}\|A^{\times}_{\times}$	$R^{\times}_{11}\|A^{\times}_{\times}$	$R^{\times}_{6}\|A^{\times}_{\times}$
f_{c4}	$R^{13}_{4,M}\|A^{4,T_{D1}:T_{D3}}_{13,B_{M,1}}$	$R^{14}_{8,H}\|A^{8,T_{D1}:T_{D2}}_{14,B_{H,1}}$	$R^{7}_{12,L}\|A^{12,T_{D2}:T_{D5}}_{7,B_{L,4}}$	$R^{1}_{16,L}\|A^{16,T_{D5}:T_{D8}}_{1,B_{L,2}}$	$R^{16}_{13,L}\|A^{13,T_{D9}:T_{D12}}_{16,B_{L,1}}$	$R^{\times}_{14}\|A^{\times}_{\times}$	$R^{13}_{15,L}\|A^{15,T_{D5}:T_{D8}}_{13,B_{L,5}}$	$R^{\times}_{7}\|A^{\times}_{\times}$

	T_{D1}	T_{D2}	T_{D3}	T_{D4}	T_{D5}	T_{D6}	T_{D7}	T_{D8}	T_{D9}	T_{D10}	T_{D11}	T_{D12}
$B_{L,1}$	1→11	1→11	1→11	1→11	5→2	5→2	5→2	5→2	13→16	13→16	13→16	13→16
$B_{L,2}$	2→5	2→5	2→5	2→5	16→1	16→1	16→1	16→1				
$B_{L,3}$	6→15	6→15	6→15	6→15				3→2	3→2	3→2	3→2	
$B_{L,4}$		12→7	12→7	12→7	12→7							
$B_{L,5}$					15→13	15→13	15→13	15→13				
$B_{M,1}$	4→13	4→13	4→13		11→3	11→3	11→3					
$B_{M,2}$	9→3	9→3	9→3									
$B_{M,3}$	10→3	10→3	10→3									
$B_{H,1}$	8→14	8→14	14→8	14→8								
$B_{WB,1}$	7→11											

T_{C1} T_{C2} T_{C3} T_{C4} T_{C5} T_{C7}

FIGURE 13. Data phase communication table using time-frequency matrix for $N = 16$.

represents a request from node p to node q for band class α and subsequent allocation from node q to p for j^{th} channel of band class α in time slots T_{Dm_1} to T_{Dm_2}. If $\times$ appears in allocation message, it means cognitive engine has denied the service in requested band class.

VIII. SIMULATION RESULTS

In this section, we present the simulation results of the proposed adaptive AMI-MAC design using physical layer cognition. Since the proposed work comprises of cross-layer PHY/MAC design, simulation results for both PHY and MAC layers are presented to validate the effectiveness of the proposed design. The simulation parameters are summarized in table 8.

Since the link parameters are directly controlled by the physical layer, we first present the working of waveform/parameter adaptation at the physical layer based on underlying channel conditions. This is shown in figure 14 with the help of SNR and throughput analysis of four types of band classes. Taking bandwidth values of low, high, medium, and wideband channels from table 8, each curve represents theoretical throughput of all modes of a band class versus E_b/N_0 values for which BER approaches to zero for each mode. The results are obtained through simulation of these modes in the Stanford University Interim (SUI) fading channel model. Referring to the horizontal dotted line shown in figure 14, if the throughput requirement of a particular node is 1000 kbps and $E_b/N_0 = 10\ dB$, CE will select mode 1 of

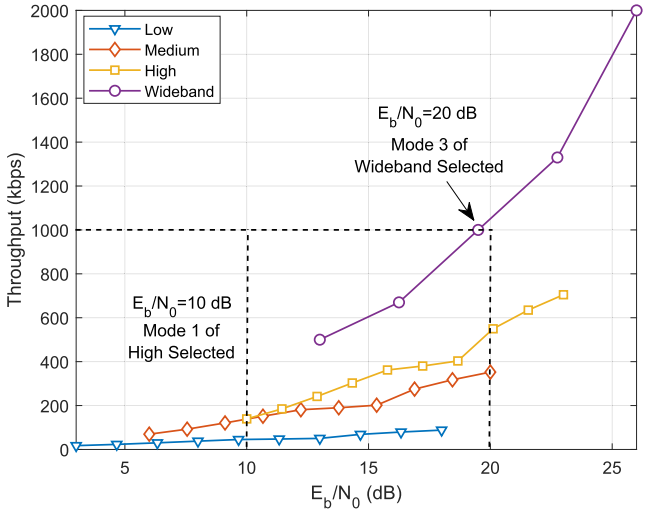

FIGURE 14. Working of the proposed cognition engine.

high bandwidth channel as the best possible option. On the other hand, if $E_b/N_0 = 20\ dB$ for the same throughput requirement, the proposed CE successfully finds mode 3 of the wideband channel, which fulfills the desired throughput requirement.

In TDM/FDM networks, control phase latency increases due to sequential transmissions that may interrupt many real-time communications, e.g., voice calls. The latency against the increasing number of nodes is depicted in figure 15. A linear increase in the control phase latency is

TABLE 8. Simulation parameters.

Parameter	Values
Bandwidth for class B_L	25 kHz
Bandwidth for class B_M	100 kHz
Bandwidth for class B_H	200 kHz
Bandwidth for class B_{WB}	1 MHz
Throughput (Mode 7) for low band class (R_L)	50.4 kbps
Throughput (Mode 7) for medium band class (R_M)	201.6 kbps
Throughput (Mode 7) for high band class (R_H)	403.2 kbps
Throughput (Mode 3) for wideband class (R_{WB})	1 Mbps
Size of control data (N_B)	40 Bytes
Duration of data slot (T_D)	12.5 ms
Duration of data slot (T_c)	6.4 ms

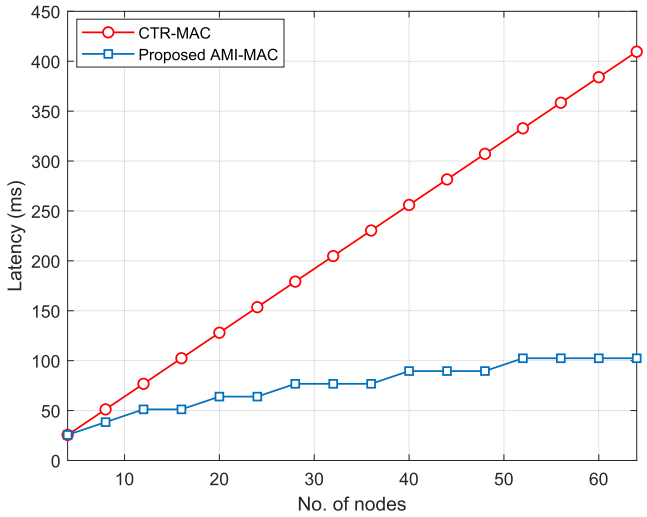

FIGURE 15. Control phase latency for CTR-MAC and AMI-MAC.

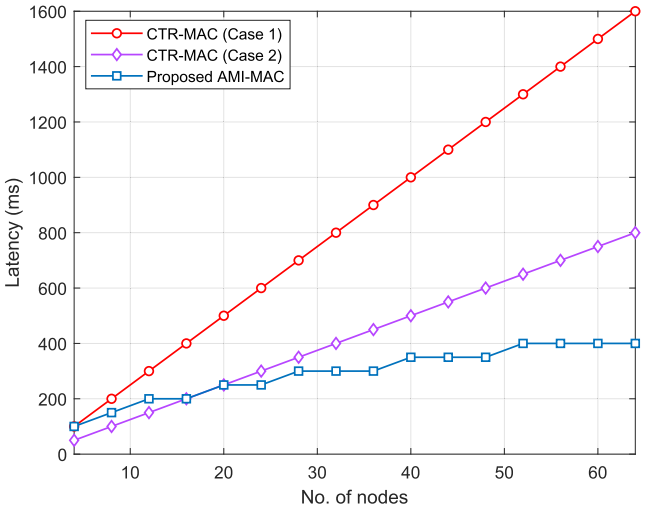

FIGURE 16. Data phase latency for CTR-MAC and AMI-MAC.

observed for CTR-MAC. On the other hand, the proposed AMI-MAC significantly reduces control phase latency due to multiple simultaneous transmissions that enable it to support networks of a much larger size.

Data phase size depends upon the network topology. In usual communications, a relatively smaller number of data slots are needed. In worst case situations, where every radio is communicating with a central node (star topology), $2N$ data slots are needed in CTR-MAC, whereas only N data slots are needed for AMI-MAC. Data phase size is usually kept tunable according to the network needs. Figure 16 represents the data phase latency of AMI-MAC compared against CTR-MAC. Case 1 is the worst case of CTR-MAC, where the number of data slots is twice the number of nodes. Case 2 is the average case of CTR-MAC, where the number of data slots is equal to the number of nodes. Apart from the advantage of control phase latency, the capability of AMI-MAC to simultaneously process multiple transmitters reduces the latency manifold.

To this point, AMI-MAC shows a significant advantage over the CTR-MAC in control phase latency due to simultaneous transmissions but also in the data phase latency due to multiple receptions. To analyze the performance in terms of network throughput, mode 3 of the wideband class is used for simulation. For an increasing number of nodes, three cases are considered, where the number of transmitting nodes is taken as 35%, 50%, and 65% of total nodes, with each sender running a constant bit rate application (1518 bytes per packet). The number of data slots required for transmission is shown in table 9 and corresponding network throughput is shown in the figure 17 for both CTR-MAC and AMI-MAC. The values for data slots given in the table are taken through simulation of a mesh network in network simulator. It is clearly shown in results that for any number of senders, the network throughput of AMI-MAC is better than the CTR-MAC. Moreover, as the number of nodes increases to a larger value, the throughput of CTR-MAC is reduced due to issues of collision and contention, and latency in the control phase of CTR-MAC.

The control phase time latency of the proposed AMI-MAC scheme is $O(\sqrt{N})$, whereas that of CTR-MAC is $O(N)$, where N is the number of radios in the network. Similarly, the computational complexity for data slot selection for both AMI-MAC and CTR-MAC is $O(\Delta N_c)$, where Δ is the number of data slots and N_c is the number of bands. However, this performance gain is at the cost of a relatively complex receiver design capable of processing multiple simultaneous signals.

TABLE 9. Number of data slots required to transmit X bytes using mode 3 of Wideband.

Nodes	35% senders		50% senders		65% senders	
	CTR-MAC	AMI-MAC	CTR-MAC	AMI-MAC	CTR-MAC	AMI-MAC
20	3	3	4	3	5	4
30	5	4	6	5	7	5
40	6	5	8	7	9	7
50	8	6	10	8	12	8
60	8	7	10	8	13	10
70	9	8	12	9	14	11
80	10	7	15	10	19	12

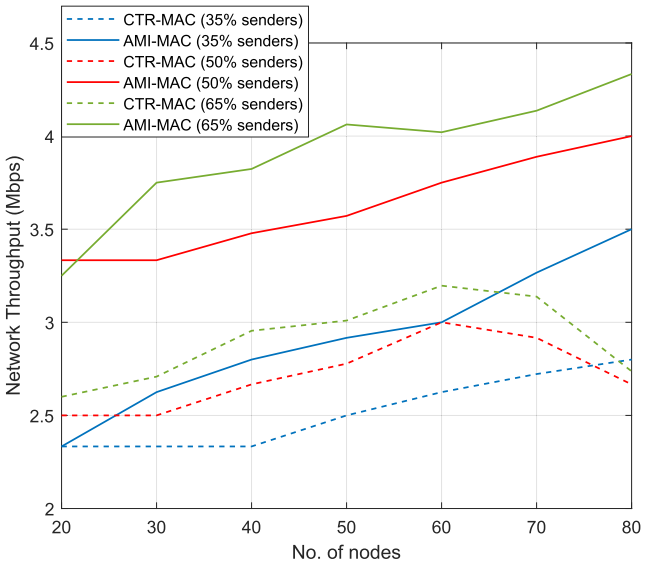

FIGURE 17. Comparison of network throughput for transmission of X bytes using mode 3 of wideband class through CTR-MAC and AMI-MAC.

IX. CONCLUSION

In this paper, we have proposed a novel cross-layer design involving adaptive multi-input medium access control (AMI-MAC) based on an intelligent cognitive engine and multiband multimode physical layer for tactical SDR networks. The aim was to achieve high throughput, improved quality of service (QoS), and adaptive range capabilities. The proposed physical layer is based on a hybrid narrowband/wideband waveform accommodating different range requirements as per demanded QoS. It operates in hybrid topology by receiving multiple signals of different bandwidths with the same configuration of wideband RF front end. Reduction in both the control and data phase latency is achieved through efficient utilization of the time and frequency resources. Results are presented to show the effectiveness of the proposed cognition engine and cross-layer design. It is shown that the proposed design shows better performance in terms of latency and network throughput over conventional tactical radio MAC.

REFERENCES

[1] T. Ulversoy, "Software defined radio: Challenges and opportunities," *IEEE Commun. Surveys Tuts.*, vol. 12, no. 4, pp. 531–550, 4th Quart., 2010.
[2] A. C. Tribble, "The software defined radio: Fact and fiction," in *Proc. IEEE Radio Wireless Symp.*, Jan. 2008, pp. 5–8.
[3] A. Zalonis, N. Miliou, I. Dagres, A. Polydoros, and H. Bogucka, "Trends in adaptive modulation and coding," *Adv. Electron. Telecommun.*, vol. 1, no. 1, pp. 104–111, 2010.
[4] K. Shahzad, S. Gulzar, M. Zeeshan, and S. A. Khan, "A novel hybrid narrowband/wideband networking waveform physical layer for multiuser multiband transmission and reception in software defined radio," *Phys. Commun.*, vol. 36, Oct. 2019, Art. no. 100790.
[5] L. Pucker, "Channelization techniques for software defined radio," in *Proc. SDR Forum Conf.*, Nov. 2003, pp. 1–6.
[6] S. Gulzar, S. A. Khan, and M. Zeeshan, "Digital hopping of narrowband waveform using wideband frontend," in *Proc. 19th Int. Conf. Adv. Commun. Technol. (ICACT)*, 2017, pp. 811–816.
[7] A. Tasic, W. A. Serdijn, and J. R. Long, "Adaptive multi-standard circuits and systems for wireless communications," *IEEE Circuits Syst. Mag.*, vol. 6, no. 1, pp. 29–37, 2006.
[8] K. S. Yeung and S. C. Chan, "The design and multiplier-less realization of software radio receivers with reduced system delay," *IEEE Trans. Circuits Syst. I, Reg. Papers*, vol. 51, no. 12, pp. 2444–2459, Dec. 2004.
[9] G. Hueber, L. Maurer, G. Strasser, R. Stuhlberger, K. Chabrak, and R. Hagelauer, "The design of a multi-mode/multi-system capable software radio receiver," in *Proc. IEEE Int. Symp. Circuits Syst.*, May 2006, p. 4.
[10] A. Tasic, S.-T. Lim, W. A. Serdijn, and J. R. Long, "Design of adaptive multimode RF front-end circuits," *IEEE J. Solid-State Circuits*, vol. 42, no. 2, pp. 313–322, Feb. 2007.
[11] G. Hueber, R. Stuhlberger, and A. Springer, "An adaptive digital front-end for multi-mode wireless receivers," in *Circuits and Systems for Future Generations of Wireless Communications*. Dordrecht, The Netherlands: Springer, 2009, pp. 249–270.
[12] R. Kwan and C. Leung, "Downlink scheduling schemes for CDMA networks with adaptive modulation and coding and multicodes," *IEEE Trans. Wireless Commun.*, vol. 6, no. 10, pp. 3668–3677, Oct. 2007.
[13] M. Zeeshan and S. A. Khan, "A novel fuzzy inference-based technique for dynamic link adaptation in SDR wideband waveform," *IEEE Trans. Commun.*, vol. 64, no. 6, pp. 2602–2609, Jun. 2016.
[14] H. S. Kim and B. Daneshrad, "Energy-aware link adaptation for MIMO-OFDM based wireless communication," in *Proc. MILCOM IEEE Mil. Commun. Conf.*, Nov. 2008, pp. 1–7.
[15] J. S. Harsini and M. Zorzi, "Link adaptation in retransmission-based cognitive radio systems," in *Proc. 6th Int. Symp. Telecommun. (IST)*, Nov. 2012, pp. 152–157.
[16] H. Chen, H. C. B. Chan, C.-K. Chan, and V. C. M. Leung, "QoS-based cross-layer scheduling for wireless multimedia transmissions with adaptive modulation and coding," *IEEE Trans. Commun.*, vol. 61, no. 11, pp. 4526–4538, Nov. 2013.
[17] A. El Shafie and A. Sultan-Salem, "Stability analysis of an ordered cognitive multiple-access protocol," *IEEE Trans. Veh. Technol.*, vol. 62, no. 6, pp. 2678–2689, Jul. 2013.
[18] A. El Shafie and T. Khattab, "On orthogonal band allocation for multiuser multiband cognitive radio networks: Stability analysis," *IEEE Trans. Commun.*, vol. 63, no. 1, pp. 37–50, Jan. 2015.
[19] X. Yue, Y. Liu, J. Wang, H. Song, and H. Cao, "Software defined radio and wireless acoustic networking for amateur drone surveillance," *IEEE Commun. Mag.*, vol. 56, no. 4, pp. 90–97, Apr. 2018.
[20] J. Vucetic and P. A. Kline, "Hybrid radio transceiver for wireless networks," U.S. Patent 6 091 715, Jul. 18, 2000.
[21] H. Yang, L. Cheng, J. Deng, Y. Zhao, J. Zhang, and Y. Lee, "Cross-layer restoration with software defined networking based on IP over optical transport networks," *Opt. Fiber Technol.*, vol. 25, pp. 80–87, Oct. 2015.

[22] H. Yang, J. Zhang, Y. Zhao, Y. Ji, J. Han, Y. Lin, and Y. Lee, "CSO: Cross stratum optimization for optical as a service," *IEEE Commun. Mag.*, vol. 53, no. 8, pp. 130–139, Aug. 2015.
[23] I. Nosheen, S. A. Khan, and U. Ali, "A cross-layer design for a multi-hop, self-healing, and self-forming tactical network," *Wireless Commun. Mobile Comput.*, vol. 2019, pp. 1–16, Apr. 2019.
[24] Rukaiya and S. A. Khan, "Self-forming multiple sub-nets based protocol for tactical networks consisting of SDRs," *IEEE Access*, vol. 8, pp. 88042–88059, 2020.
[25] I. Nosheen, S. A. Khan, and F. Khalique, "A mathematical model for cross layer protocol optimizing performance of software-defined radios in tactical networks," *IEEE Access*, vol. 7, pp. 20520–20530, 2019.
[26] C.-E. Sundberg, "Continuous phase modulation," *IEEE Commun. Mag.*, vol. 24, no. 4, pp. 25–38, Apr. 1986.
[27] S. Kundrapu, S. I. Dutt V. B. S., N. K. Koilada, and A. C. Raavi, "Characteristic analysis of OFDM, FBMC and UFMC modulation schemes for next generation wireless communication network systems," in *Proc. 3rd Int. Conf. Electron., Commun. Aerosp. Technol. (ICECA)*, Jun. 2019, pp. 715–721.
[28] I. B. F. de Almeida, L. L. Mendes, J. J. P. C. Rodrigues, and M. A. A. da Cruz, "5G waveforms for IoT applications," *IEEE Commun. Surveys Tuts.*, vol. 21, no. 3, pp. 2554–2567, 3rd Quart., 2019.
[29] A. J. Tiwana and M. Zeeshan, "Parametric analysis of FBMC/OQAM under SUI fading channel models," in *Proc. 22nd Int. Conf. Adv. Commun. Technol. (ICACT)*, Feb. 2020, pp. 207–211.
[30] A. F. Isnawati, V. O. Citra, and J. Hendry, "Performance analysis of audio data transmission on FBMC—Offset QAM system," in *Proc. IEEE Int. Conf. Ind. 4.0, Artif. Intell., Commun. Technol. (IAICT)*, Jul. 2019, pp. 81–86.
[31] A. I. Perez-Neira, M. Caus, R. Zakaria, D. Le Ruyet, E. Kofidis, M. Haardt, X. Mestre, and Y. Cheng, "MIMO signal processing in offset-QAM based filter bank multicarrier systems," *IEEE Trans. Signal Process.*, vol. 64, no. 21, pp. 5733–5762, Nov. 2016.

KASHIF SHAHZAD received the B.Sc. degree in electrical engineering from the University of Engineering and Technology, Taxila, Pakistan, in 2004, and the master's degree in electrical engineering from the College of Electrical and Mechanical Engineering, National University of Sciences and Technology, Pakistan, in 2010, with major in signals processing and wireless communications, where he is currently pursuing the Ph.D. degree in electrical engineering. He has a vast experience in research and development for over 13 years in the field of embedded software development and digital signal processing. His research interests include embedded systems and signal processing for communications.

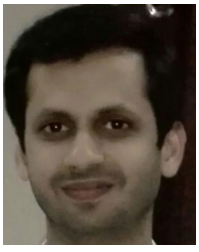

MUHAMMAD UMAR FAROOQ received the master's degree in computer science from Quaid-i-Azam University, Pakistan, the master's degree in software engineering from the National University of Sciences and Technology, Pakistan, and the Ph.D. degree in computer science from the University Politehnica of Bucharest, Romania. He is currently an Assistant Professor of computer and software engineering with the College of Electrical and Mechanical Engineering, National University of Sciences and Technology. He is an inventor of one awarded U.S. patent, a reviewer of several international conferences and journals, and the author of several international publications. His research interests include routing and MAC protocols for wireless ad hoc networks, delay tolerant networks, and the Internet of Things.

MUHAMMAD ZEESHAN (Member, IEEE) received the Ph.D. degree in electrical engineering with specialization in wireless communications from the College of Electrical and Mechanical Engineering, National University of Sciences and Technology (NUST), Pakistan, in 2015. From July 2010 to March 2016, he was with the Center for Advanced Research in Engineering (CARE), Pakistan, first as a Senior Design Engineer, and then as a Member of Technical Staff, in July 2014. Since 2010, he has been actively involved in research and development in the field of software defined radio (SDR), wideband waveform design, time/frequency synchronization algorithms, and radar signal processing. In March 2016, he joined the faculty of the College of Electrical and Mechanical Engineering, National University of Sciences and Technology (NUST), Pakistan, where he is currently an Assistant Professor of wireless communications with the Department of Electrical Engineering. At this department, he is also heading the Cognitive Radio & Wireless Communications (CoRWiC) research group. He has a number of international journal and conference publications. His research interests include SDR waveform development, physical layer design, synchronization techniques, and digital design of wireless communication systems. He is a Reviewer of the IEEE TRANSACTIONS ON COMMUNICATIONS, IEEE ACCESS, and *Wireless Personal Communications*.

SHOAB AHMED KHAN received the Ph.D. degree in electrical and computer engineering from the Georgia Institute of Technology, Atlanta, GA, USA, in 1995. He has been actively involved in research and development, has authored over 200 publications in international conferences and journals, and holds six U.S. patents. He has 17 years of industrial experience in companies, like Scientific Atlanta, Picture Tel, Cisco Systems, and Avaz Networks. As a Chief Architect, he designed a high-density media processor for a carrier-class voice processing system. He is currently a Professor and the Head of the Department of Computer Engineering with the College of Electrical and Mechanical Engineering, National University of Sciences and Technology, Pakistan. He is also the Founder of the Center for Advanced Studies in Engineering and the Center for Advanced Research in Engineering, two prominent organizations working for the promotion of research and development in Pakistan. He was a recipient of the National Education Award 2001 in the category of Outstanding Services to Science and Technology, the NCR National Excellence Award in the category of IT Education, the prestigious Cisco System Research Grant, and ICT R&D and PTCL R&D research findings.